ISSN 1936-5330



The Dynamic Distribution in the Fixed Cost Model: An Analytical Solution

Jonathan J. Adams

August 2026
RWP 26-07
https://doi.org/10.18651/RWP2026-07



The Dynamic Distribution in the Fixed Cost Model: An Analytical Solution*

Jonathan J. Adams
Federal Reserve Bank of Kansas City

July 24, 2026

WORKING PAPER: Link to Most Current Version

Abstract

I derive an analytical solution to the Kolmogorov forward equation for fixed cost models. This is a challenging PDE because the dynamic distribution depends on the flow of resetting agents, which is endogenously determined by the distribution itself. I show that there is a shortcut that allows the reset flow to be derived without first finding the entire distribution of agents. This shortcut is also valuable because many aggregate variables can be written in terms of the reset flow alone. Steady-state conditional adjustment behavior recovers the entire marginal reset-flow response to a common state shift. As an example, I solve an investment model with fixed costs of adjustment and study the effects of increased productivity growth. Aggregate dynamics can be derived from a one-dimensional weighted distribution of capital gaps. Because of adjustment frictions, the shock causes a boom-lull investment pattern whose shape depends on the shock size.

JEL Codes: C60, E22, E32

Keywords: Fixed Costs, Investment, Nonlinear Dynamics, Large Shocks, State Dependence, Kolmogorov Forward Equations, Impulse Response Functions

*Website: www.jonathanjadams.com Email: adamsjonathanj@gmail.com. I am grateful for constructive feedback from Fernando Alvarez, David Argente, Philip Barrett, Saki Bigio, Andres Blanco, Mishel Ghassibe, Francesco Lippi, and Luminita Stevens, as well as conference participants at the 2025 Summer Workshop on Money, Banking, Payments, and Finance at the Bank of Canada. The views expressed herein are those of the author and do not necessarily represent the views of the Federal Reserve Bank of Kansas City or the Federal Reserve System.

1 Introduction

Many economic decisions require paying fixed costs. The microeconomics of these decisions are well understood. But the macroeconomics of fixed costs are challenging to study, because it often requires keeping track of an infinite-dimensional state variable: the dynamic distribution of agents. The evolution of the distribution is governed by a partial differential equation (PDE), the *Kolmogorov Forward Equation* (KFE).[1] The solution to this equation has proven difficult to characterize analytically because it depends on the flow of resetting agents, which itself is determined endogenously from the dynamic distribution. As a result of this nonlinear feedback, theorists rely on perturbation methods or other approximations to characterize aggregate behavior.

To address these challenges, I derive an analytical solution for the dynamic distribution in a canonical fixed cost model. The key insight is that the endogenous flow of resetting agents can be determined without first solving for the dynamic distribution of states. This circumvents the challenging endogenous feedback. Once the time path of the "reset flow" is known, the dynamic distribution is found using a standard PDE solution. But the reset flow is even more valuable: many macroeconomic variables that depend on the distribution can be calculated using the reset flow alone, avoiding the need to calculate the dynamic distribution at all.

The results in this paper are useful for studying aggregate shocks, because the KFE determines how the distribution of agents responds over time, and macroeconomic variables such as output or inflation are functions of this distribution. The general model describes economic decisions subject to a wide variety of frictions. This type of fixed cost model – with aggregate shocks and a dynamic distribution governed by a KFE – appears in many examples, including: investment adjustment costs (Baley and Blanco, 2021), hiring and firing costs (Elsby and Michaels, 2019), information acquisition costs (Alvarez et al., 2018), wage renegotiation costs (Blanco and Drenik, 2023), and famously menu costs (Golosov and Lucas Jr., 2007).

This is an advance relative to existing methods. Historically, fixed cost models employed clever assumptions so that the distribution was not a necessary aggregate state variable (Caplin and Spulber, 1987; Caplin and Leahy, 1997). In recent years, theorists have made considerable progress in understanding the macroeconomics of

[1] Physicists use the term "Fokker-Planck equation", which is a specific type of KFE. But the Kolmogorov terminology is more common in economics, so I use it as well.

fixed cost models by utilizing a variety of approximations.[2] Many researchers employ perturbation methods around the steady-state distribution. This approach yields valid conclusions for small shocks and is convenient for characterizing linear relationships between aggregate variables (e.g. Gertler and Leahy, 2008; Auclert et al., 2024) or approximating their dependence on the distribution (e.g. Alvarez and Lippi, 2014; Alvarez et al., 2023). However, numerical solutions to the nonlinear model demonstrate that conclusions regarding small shocks do not necessarily generalize (Golosov and Lucas Jr., 2007; Cavallo et al., 2024). Thus, one value of the analytical solution is for studying large shocks. Furthermore, the reset flow representation is especially useful in settings where endogenous "reinjection" cannot be ignored, such as models featuring asymmetry, drift, or aggregates that depend on even moments.[3]

The value of the analytical solution is not limited to computation; it can reveal new theoretical insights. To demonstrate, I derive a new *functional sufficient statistic* for the marginal effects of an aggregate shock that shifts the distribution. The sufficient-statistic literature following Alvarez et al. (2016) studies the cumulative impulse response (CIR) to this shock and characterizes how it relates to the distribution of adjustments in the steady state. The analytical solution allows me to expand on this strategy. I show that the reset flow's entire marginal impulse response function (IRF) can be expressed in terms of two objects measurable in the steady state: the reset-time density for a new spell and the average slope of the conditional survival function. Moreover, this result applies to a generalized model that allows the diffusion, drift, and reset hazard to depend on the state. The marginal IRFs of other aggregates then follow linearly from the reset-flow IRF.

As an example, I demonstrate the analytical solution in a standard investment model with fixed costs of adjustment. The firms' (S, s) strategies are well known; the contribution is to aggregation, where again the reset flow representation reveals new insights. I show that the IRFs of detrended aggregate capital and output do not require the joint distribution of capital and productivity. Rather, they are determined

[2]The approximations discussed in this section have been useful for theoretical analysis of fixed cost models. Further approximations are used for quantitative analysis; for example, Midrigan (2011) and many other papers use the Krusell and Smith (1998) method to encode the infinite-dimensional distribution.

[3]Alvarez and Lippi (2022) previously made substantial progress by assuming there is no "reinjection", i.e., agents leave the distribution after resetting. This method is useful for calculating IRFs of odd moments in models with symmetric inaction regions and no drift (e.g., no trend inflation or productivity growth) because the KFE reduces to the classic heat equation.

by a one-dimensional productivity-weighted distribution of capital gaps, which follows a KFE and can be solved via the reset-flow shortcut. I apply this result to study the arrival of artificial intelligence (AI), modeled as a permanent increase in productivity growth. Although the stationary distribution barely changes, fixed adjustment costs generate distorted transition dynamics: an immediate investment boom followed by an extended lull. Moreover, the analytical solution reveals that the depth of the lull depends nonlinearly on the shock size.

The next section describes the canonical fixed cost model. Section 3 derives the solution. Section 4 demonstrates how to express aggregate dynamics in terms of the reset flow. Section 5 derives the functional sufficient-statistic result for marginal common state shifts. Section 6 applies the solution to a fixed-cost investment model. Section 7 concludes.

2 The Fixed Cost Model

This section introduces the canonical fixed cost model, abstracting from decision-making microfoundations to focus on aggregation and the dynamic distribution.[4]

I develop the analytical solution in three steps. This section defines the reset flow and Lemma 1 states the KFE conditional on that flow. Then Theorem 1 uses the Green's function to solve directly for the reset flow, after which the distribution can be recovered. Finally Theorem 2 shows that many aggregate dynamics can be calculated from the reset flow alone, without first recovering the distribution.

There is a continuum of agents i; at any time t, each agent is characterized by a state variable $x_i(t)$. Each agent's state variable follows a diffusion:

$$dx_i(t) = \mu dt + \sigma dW_i(t) \tag{1}$$

where $W_i(t)$ is Brownian motion that is independent across agents, and μ captures a common trend. For notational clarity, I drop the i and t arguments henceforth.

When an agent's state is sufficiently low ($x \leq 0$) or sufficiently high ($x \geq \bar{x}$), it is willing to pay a fixed cost and reset its state to $x = x^*$. The interval $[0, \bar{x}]$ with $0 < x^* < \bar{x}$ is assumed to be constant.[5] Agents also randomly reset at rate $\eta \geq 0$,

[4] See Stokey (2008) for a textbook treatment.

[5] Because x^* must be in the interior, this rules out models where agents exit one side of a region to reappear at the other, such as Caplin and Spulber (1987).

leaving the distribution and reentering at $x = x^*$.

The distribution of agents' states is $h(x,t)$, a function on $x \in [0, \bar{x}]$ and $t \geq 0$. Solving the fixed cost model entails finding the function $h(x,t)$ that satisfies a number of conditions:

1. The distribution satisfies the KFE:[6]

$$\partial_t h(x,t) = \gamma \partial_x^2 h(x,t) - \mu \partial_x h(x,t) - \eta h(x,t) \tag{2}$$

   on the interval $[0, x^*) \cup (x^*, \bar{x}]$, where $\gamma \equiv \frac{\sigma^2}{2}$.

2. The *continuity condition*: while $h(x,t)$ might not be differentiable in x at x^*, it must be continuous for $t > 0$.

3. The bounds 0 and $\bar{x}$ are absorbing barriers, implying the Dirichlet boundary conditions

$$h(0,t) = 0 \qquad h(\bar{x},t) = 0$$

4. The distribution is consistent with the initial condition

$$h(x,0) = \phi(x)$$

   where $\phi(x)$ is a probability measure, possibly with point masses.

5. Probability is conserved, i.e., for all t,

$$\int_0^{\bar{x}} h(x,t)\, dx = 1$$

This structure has been used to study economic inaction in a wide variety of settings.

The model differs from a standard diffusion because agents who leave through either boundary or reset randomly immediately reenter at x^*. Define the *reset flow* $F(t)$ as

$$F(t) \equiv \gamma \partial_x h(0,t) - \gamma \partial_x h(\bar{x},t) + \eta \tag{3}$$

The first two components capture the probability flow across the boundaries, while η is the flow of random adjustments.[7] These agents reenter the distribution at x^*,

[6] See (Stokey, 2008, Section 3.3) for an introduction to the KFE.

[7] In this paper, derivatives at boundaries denote one-sided derivatives from the interior.

creating a point-like source where probability enters at rate $F(t)$.

Lemma 1 formalizes how the reset flow definition follows from the conservation assumption $\int_0^{\bar{x}} h(x,t)\,dx = 1$, extends the KFE to the entire inaction region, and gives all the conditions as a standard PDE problem.

Lemma 1. *Conditional on the reset flow $F(t)$, the model is given by the following PDE problem for $x \in [0, \bar{x}]$ and $t \geq 0$:*

$$\partial_t h(x,t) = \gamma \partial_x^2 h(x,t) - \mu \partial_x h(x,t) - \eta h(x,t) + \delta(x - x^*)F(t)$$

$$h(0,t) = 0 \qquad h(\bar{x},t) = 0$$

$$h(x,0) = \phi(x)$$

where $\delta(x - x^*)$ is the Dirac delta.

Proof: Appendix A.1

2.1 Economic Environments

The state variable x typically represents a gap between a past choice and an ideal target. Gaps evolve stochastically, and when the gap gets large enough, agents are willing to pay a fixed cost and reset to x^*: an (S, s) model. This structure applies to a wide variety of settings.

A classic example is investment, for which inaction and large discrete adjustments are observed in the data. The model I explore in Section 6 is a special case of the investment model studied and estimated by Baley and Blanco (2021).

Sticky prices are another common example, where x represents the gap between a firm's current and desired price. Menu costs generate the inaction region; following Golosov and Lucas Jr. (2007), Nakamura and Steinsson (2010), and others, Alvarez and Lippi (2022) provide an example of the continuous-time formulation.

With fixed hiring and firing costs, x is an employment gap, and firms adjust employment only when it is sufficiently far from its target (Elsby and Michaels, 2019). Inventory management also has an (S, s) structure: x is an inventory of finished products, which declines stochastically until a fixed ordering cost is paid and the stock is replenished (Fisher and Hornstein, 2000). In durable replacement decisions,

x can measure the age or condition of a machine that is costly to fix or replace (Cooper et al., 1999).

Rational inattention is another friction that can create inaction. When an agent's state is close to its target, the gain from acquiring information and reconsidering its choice is small; as the gap grows, more frequent review becomes valuable. Woodford (2009) applies this idea to state-dependent price-setting, and Alvarez et al. (2022) show that information-acquisition costs imply that the KFE includes a generalized adjustment hazard. This does not necessarily fit in the baseline framework, where the random reset rate is a constant η. However, some results still generalize, as I discuss next.

2.2 Generalization and Caveats

How general is this fixed cost model? The constant coefficients in equation (2) are a common case. But what if the coefficients are allowed to be state-dependent? Assume $\gamma(x) > 0$ and $\eta(x) \geq 0$, with the coefficients sufficiently regular. Then the more general KFE becomes

$$\partial_t h(x,t) = \partial_x^2 \left(\gamma(x)h(x,t)\right) - \partial_x \left(\mu(x)h(x,t)\right) - \eta(x)h(x,t) + \delta(x - x^*)F(t) \tag{4}$$

while the mass-preserving flow becomes

$$F(t) = \partial_x \left(\gamma(x)h(x,t)\right)\big|_{x=0} - \partial_x \left(\gamma(x)h(x,t)\right)\big|_{x=\bar{x}} + \int_0^{\bar{x}} \eta(x)h(x,t)\,dx \tag{5}$$

Without constant coefficients, the exact closed-form expressions I derive no longer apply. But the main practical insights still do: it is sufficient to find the reset flow $F(t)$ in order to characterize the solution. Theorems 1, 2, and 3 still hold without invoking the constant-coefficient expressions.

A real caveat is that the model assumes constant inaction boundaries. This is a feature of many models such as the fixed-cost investment example in Section 6. In other cases, it is merely a simplification.[8] The current approach *can* be used to address shocks that have permanent effects on the boundaries; Section 6.3 is an

[8]Particularly in menu cost models, it is common to assume that shocks do not affect the inaction region and that firms follow steady-state decision rules. Alvarez and Lippi (2014) and Cavallo et al. (2024) show that this is an accurate approximation for standard parameters.

example. But models with truly dynamic boundaries require additional work. To address this, Adams (2026) builds on insights in the present paper to solve the full mean field game, including optimal dynamic boundaries.

3 Solution

The model is a standard linear PDE conditional on the reset flow $F(t)$. This section first uses the Green's function to describe that conditional solution, then solves directly for the reset flow.

3.1 The Green's Function

A Green's function is a distributional IRF. $G(x, y, t)$ gives the density over x at horizon t generated by a unit mass initially located at y, while that mass follows the homogeneous KFE. Solutions for arbitrary initial densities and reset flows can then be constructed by varying the inputs y and t.

To build the Green's function, let $\mathcal{K}$ and $\mathcal{K}^\dagger$ define the Kolmogorov operator and its adjoint. $\mathcal{K}$ applies the right-hand side of the KFE to a function; in the constant-coefficient model it is thus

$$\mathcal{K} \equiv \gamma\partial_x^2 - \mu\partial_x - \eta \qquad \mathcal{K}^\dagger \equiv \gamma\partial_x^2 + \mu\partial_x - \eta$$

Let $\psi_n^r(x)$ and $\psi_n^\ell(x)$ denote its right and left eigenfunctions, respectively, with eigenvalue $-\lambda_n$ and absorbing boundary conditions:

$$\mathcal{K}\psi_n^r(x) = -\lambda_n\psi_n^r(x) \qquad \mathcal{K}^\dagger\psi_n^\ell(x) = -\lambda_n\psi_n^\ell(x)$$

Scale the left and right eigenfunctions so that the product of each matching pair integrates to one. $n = 1, 2, \ldots$ indexes the eigenvalues of the Kolmogorov operator. The Green's function is their infinite sum:

$$G(x, y, t) \equiv \sum_{n=1}^{\infty} \psi_n^r(x)\, \psi_n^\ell(y)\, e^{-\lambda_n t} \tag{6}$$

Supplemental Appendix B gives the exact closed-form expressions for λ_n, $\psi_n^\ell(x)$, and $\psi_n^r(x)$.

The Green's function is a powerful and versatile tool, as Property 1 shows. If the reset flow is known, then the Green's function can be used to write the full dynamic distribution. Alternatively, Theorems 1 and 2 use the Green's function to derive aggregate dynamics directly without first constructing the distribution.

Property 1. *Given $F(t)$, the Green's function solution to the KFE is*

$$h(x,t) = \int_0^{\bar{x}} \phi(y)\, G(x,y,t)\, dy + \int_0^t F(\tau)\, G(x,x^*,t-\tau)\, d\tau \tag{7}$$

The first term propagates the initial density. The second adds the distributions generated by cohorts that reset at each earlier time τ. This is the standard Green's function solution for a non-homogeneous linear PDE.[9]

3.2 The Reset Flow

Equation (7) gives the distribution conditional on $F(t)$, but there is a feedback: $F(t)$ itself is endogenously determined by the distribution. This section's central result is that the reset flow can instead be determined in isolation without first solving for $h(x,t)$.

In continuous time, it is often useful to work in the frequency domain rather than the time domain. The following theorem gives the *Laplace transform* $\hat{F}(s)$ of the flow function. The Laplace transform of a function is defined by

$$\hat{F}(s) \equiv \mathcal{L}\{F\}(s) = \int_0^\infty F(t)\, e^{-st}\, dt$$

Theorem 1 (Reset Flow)**.** *The Laplace transform of the reset flow is*

$$\hat{F}(s) = \frac{\hat{A}(s)}{1-\hat{B}(s)} \tag{8}$$

where

$$\hat{A}(s) \equiv \sum_{n=1}^{\infty} \frac{\theta_n\, a_n}{s+\lambda_n} \qquad \hat{B}(s) \equiv \sum_{n=1}^{\infty} \frac{\theta_n\, b_n}{s+\lambda_n}$$

[9] See (Polyanin, 2001, Sec. 0.4.2–4, 0.7.1–2, and 3.1.5) for equation (6), (7), and the constant-coefficient form, respectively.

and

$$
\begin{aligned}
a_n &\equiv \int_0^{\bar{x}} \psi_n^{\ell}(y)\, \phi(y)\, dy \\
b_n &\equiv \psi_n^{\ell}(x^*) \\
\theta_n &\equiv \gamma(0)(\psi_n^r)'(0) - \gamma(\bar{x})(\psi_n^r)'(\bar{x}) + \int_0^{\bar{x}} \eta(x)\psi_n^r(x)\, dx
\end{aligned} \tag{9}
$$

Proof: Appendix A.2

Theorem 1 is written to apply to Section 2.2's generalized model. For the constant-coefficient baseline, Supplemental Appendix B gives closed-form expressions for a_n, b_n, and θ_n.

The coefficient θ_n gives the total reset flow generated by eigenmode n, combining boundary and random resets. The function $\hat{A}(s)$ captures resets out of the initial distribution, while $\hat{B}(s)$ captures resets out of the reinjections at x^*. In the frequency domain, convolution becomes multiplication, so the reset flow satisfies $\hat{F}(s) = \hat{A}(s) + \hat{B}(s)\,\hat{F}(s)$. Theorem 1 solves this scalar equation directly, without using the entire distribution $h(x,t)$.

3.3 The Distribution

Once the reset flow is known, the distribution follows from Property 1. Corollary 1 states the solution.

Corollary 1. *The unique dynamic distribution is given by equation* (7)*, with* $F(t)$ *determined by Theorem 1. Thus, its Laplace transform is*

$$
\begin{aligned}
\hat{h}(x,s) &= \sum_{n=1}^{\infty} \psi_n^r(x)\, \frac{a_n + b_n\, \hat{F}(s)}{s + \lambda_n} \\
&= \sum_{n=1}^{\infty} \psi_n^r(x)\, \frac{\hat{A}(s)\, b_n + \left(1 - \hat{B}(s)\right)\, a_n}{\left(1 - \hat{B}(s)\right)\,(s + \lambda_n)}
\end{aligned}
$$

Proof: Appendix A.3

Corollary 1 contains all the objects needed to compute $h(x,t)$. The transform $\hat{h}(x,s)$ can be easily inverted to the time domain using a partial fraction expansion.Still, the next section shows that the distribution need not be computed at all for many aggregate outcomes.

4 Using the Flow Function to Calculate Aggregate Dynamics

The dynamics of aggregate variables depend on the distribution $h(x,t)$. In many cases, an aggregate variable $Z(t)$ (or some transformation thereof) requires integrating over the distribution by

$$Z(t) = \int_0^{\bar{x}} f_Z(x)\, h(x,t)\, dx \tag{10}$$

for some function $f_Z(x)$. Section 4.3 will discuss some common examples.[10]

Equation (7) implies that $Z(t)$ can be calculated from $F(t)$ without first constructing $h(x,t)$.

4.1 Frequency-Domain Macroeconomic Aggregates

The shortcut is cleanest in the frequency domain: Theorem 2 shows that $\hat{Z}(s)$ is linear in $\hat{F}(s)$, while Corollary 2 gives the equivalent time-domain representation.

Theorem 2 (Linearity)**.** *The Laplace transform $\hat{Z}(s)$ of an aggregate variable $Z(t)$ given by equation* (10) *is linear in the Laplace transform of the reset flow $\hat{F}(s)$:*

$$\hat{Z}(s) = \hat{A}^Z(s) + \hat{B}^Z(s)\,\hat{F}(s)$$

for

$$\hat{A}^Z(s) \equiv \sum_{n=1}^{\infty} \frac{\theta_n^Z\, a_n}{s+\lambda_n} \qquad \hat{B}^Z(s) \equiv \sum_{n=1}^{\infty} \frac{\theta_n^Z\, b_n}{s+\lambda_n}$$

where a_n and b_n are given by Theorem 1 and

$$\theta_n^Z \equiv \int_0^{\bar{x}} f_Z(x)\, \psi_n^r(x)\, dx$$

Proof: Appendix A.4

The $\hat{A}^Z(s)$ term captures how the initial distribution affects the aggregate variable, while the $\hat{B}^Z(s)$ term captures the effect of the dynamic flow of resets. This is

[10] The representation in equation (10) also reveals the relationship with Alvarez and Lippi (2022). When $\bar{x} = 2x^*$ and $f_Z(x)$ is an odd function, the IRF can be found easily by solving the model without "reinjection". Without reinjection, the reset flow is $F(t) = 0$, and the PDE reduces to a standard homogeneous heat equation.

straightforward to see in the time-domain expression for $Z(t)$, which is an immediate corollary:

Corollary 2 (Time-Domain Aggregation)**.** *The aggregate variable $Z(t)$ is*

$$Z(t) = A^Z(t) + \int_0^t F(\tau)\, B^Z(t-\tau)\, d\tau$$

Proof: Follows from Theorem 2, where $\hat{A}^Z(s)$ and $\hat{B}^Z(s)$ are Laplace transforms of $A^Z(t)$ and $B^Z(t)$.

4.2 Impulse and Cumulative Responses

Theorem 2 showed that macroeconomic aggregates are easily calculated in the frequency domain, where $\hat{Z}(s)$ is linear in the reset flow. This section demonstrates how to convert $\hat{Z}(s)$ into macroeconomic objects that are typically reported: the IRF and CIR.

A convenient property of the frequency domain is that $\hat{Z}(s)$ can be treated as an infinite-order polynomial fraction and thus easily inverted to the time domain.[11] If its poles are simple, denote its partial fraction expansion by

$$\hat{Z}(s) = \sum_{j=0}^{\infty} \frac{\xi_j^Z}{s + \rho_j^Z} \tag{11}$$

As a convention, let the index $j = 0$ denote the zero pole, i.e., $\rho_0^Z = 0$. Therefore $\xi_0^Z = \overline{Z}$, the long-run value of the aggregate variable $Z(t)$.

Corollary 3 gives the IRF in terms of the partial fraction expansion. It also gives the CIR, which many economists use to summarize the effects of shocks in continuous-time models.

Corollary 3 (Impulse Response Function)**.** *The impulse response function $IRF^Z(t) \equiv Z(t) - \overline{Z}$ is*

$$Z(t) - \overline{Z} = \sum_{j=1}^{\infty} \xi_j^Z\, e^{-\rho_j^Z t}$$

[11] This is true if $f_Z(x) \in \mathcal{C}^1$. Any finite truncation of the eigenfunction sum used for computation implies that $\hat{Z}(s)$ in the computer is necessarily rational and thus has an ordinary finite partial-fraction expansion. Differentiable $f_Z(x)$ ensures that the eigenfunction weights decay sufficiently for a finite truncation to converge for $t > 0$.

for $t > 0$, and the cumulative impulse response CIR^Z is

$$CIR^Z \equiv \int_0^\infty \left[Z(t) - \overline{Z}\right] dt = \sum_{j=1}^{\infty} \frac{\xi_j^Z}{\rho_j^Z}$$

where ξ_j^Z and ρ_j^Z correspond to the partial fraction expansion in equation (11).

Proof: Appendix A.5

Corollary 3 is immediately useful in settings where $Z(t)$ itself is relevant (e.g., investment models). In other cases, the aggregate variable of interest must first be transformed into a $Z(t)$ that satisfies equation (12) (e.g., the Golosov-Lucas output gap).

4.3 Examples of Aggregating Functions

In this section, I discuss common examples of aggregating functions $f_Z(x)$. Supplemental Appendix B.2 derives their associated θ_n^Z series.

The Average Exponential State: Many aggregate variables $Z(t)$ depend on an average exponential function of the state:

$$Z(t) = \int_0^{\bar{x}} e^{\epsilon x} h(x,t)\, dx \tag{12}$$

for some ϵ. For example, in Golosov and Lucas Jr. (2007) x is the log markup gap, and evaluating this integral gives an output gap (raised to some power). In investment models, x is the log capital-productivity ratio, and evaluating this integral gives the average capital-productivity ratio. Section 6.2 shows that a productivity-weighted density can instead be used to recover aggregate capital.

The Average State: In some cases, aggregate variables $Z(t)$ depend on the average state ($f_Z(x) = x$):

$$Z(t) = \int_0^{\bar{x}} x h(x,t)\, dx \tag{13}$$

It is also common to use the average state as an approximation of a nonlinear function. For example, in the menu cost model studied by Alvarez et al. (2024), the aggregate output gap is calculated as proportional to the average markup gap.

The Squared State: It may be valuable to calculate the dynamics of higher-order moments, for example, to study the dynamics of misallocation. Many applications

depend on the average squared state ($f_Z(x) = x^2$):

$$Z(t) = \int_0^{\bar{x}} x^2 h(x,t)\, dx \tag{14}$$

For example, in Baley and Blanco (2026) and Adams et al. (2025), the average squared state measures capital misallocation. In Cavallo et al. (2023), it captures welfare costs of inflation due to misallocation.

5 A Functional Sufficient Statistic

There is another value of the analytical solution: it can uncover new properties of the model, as this section demonstrates.

The sufficient-statistic literature uses steady-state adjustment statistics to characterize how small shocks to the distribution affect aggregates in fixed cost models. For practical reasons, this strategy has focused on the CIR of the average state in idealized settings. For example, Alvarez et al. (2016) derive the CIR following a monetary shock in a constant-coefficient menu cost model with zero drift and a symmetric inaction region. Subsequent work allows for nonzero drift and asymmetric policies (Baley and Blanco, 2021), and for generalized state-dependent hazards (Alvarez et al., 2022).

Existing results summarize an IRF by its cumulative effect, but the solution in Section 3 enables new possibilities. Theorem 3 extends the prior approaches by deriving a *functional sufficient statistic*: the entire marginal IRF of the reset flow can be expressed in terms of steady-state objects. This result is *functional* because its empirical inputs are functions. It is a *sufficient statistic* because steady-state objects determine the IRF in Section 2.2's generalized model without needing to solve the model or identify its parameters.

The necessary empirical objects are derived from the conditional survival function $S(t \mid y)$, which is the probability that an agent beginning at y has not reset by time t. It is related to the Green's function by

$$S(t \mid y) \equiv \int_0^{\bar{x}} G(x,y,t)\, dx \tag{15}$$

The corresponding conditional reset-time density is

$$m(t \mid y) \equiv -\partial_t S(t \mid y) \tag{16}$$

Define the reset density after adjustment and the steady-state average conditional survival slope by

$$\begin{aligned} \mathbf{m}(t) &\equiv m(t \mid x^*) \\ \acute{\mathbf{S}}(t) &\equiv \int_0^{\bar{x}} \partial_y S(t \mid y) \bar{h}(y)\, dy \end{aligned} \tag{17}$$

which are the building blocks of the functional sufficient statistic and are plausibly measurable in panel datasets of adjustments such as those used by Caballero et al. (1995), Baley and Blanco (2021), or Alvarez et al. (2024).

The functional sufficient statistic applies to an aggregate shock that increases the state of all agents. In Section 6's investment model, this represents a negative productivity shock. The inaction region is assumed to remain fixed; this is true in the investment model and is a common approximation in some other settings. Specifically, at $t = 0$ an unanticipated shock increases every agent's state by Δ. Let $F(t; \Delta)$ denote the resulting reset flow and define its marginal IRF as

$$F^{\Delta}(t) \equiv \left. \frac{\partial F(t; \Delta)}{\partial \Delta} \right|_{\Delta = 0}$$

Theorem 3 (Functional Sufficient Statistic)**.** *The reset flow's marginal IRF satisfies*

$$F^{\Delta}(t) = -\partial_t \acute{\mathbf{S}}(t) + \int_0^t \mathbf{m}(t - \tau) F^{\Delta}(\tau)\, d\tau \tag{18}$$

for $t > 0$, with Laplace transform

$$\hat{F}^{\Delta}(s) = \frac{-s \hat{\acute{\mathbf{S}}}(s)}{1 - \hat{\mathbf{m}}(s)} \tag{19}$$

Proof: Appendix A.6

The first term in equation (18) captures how the common shift changes the timing of the next reset among inaction spells already underway. The convolution term accounts for the flow from agents who reenter at x^*. Compared with CIR sufficient

statistics, which require only a few steady-state moments, richer adjustment information (i.e., $\mathbf{m}(t)$ and $\acute{\mathbf{S}}(t)$) is required to recover the full reset-flow IRF. Thus, the theorem complements the prior literature: introducing additional data yields additional results.

The reset-flow analysis in Section 3 is essential to the proof of Theorem 3. Theorem 2 then maps the resulting marginal flow IRF into aggregate dynamics without requiring a separate sufficient-statistic derivation for each aggregate.

6 Example: Fixed Costs of Investment and the Advent of AI

To demonstrate the usefulness of the analytical solution, this section presents a classic example: capital investment with fixed costs of adjustment. I analyze a standard model, reminiscent of Caballero and Engel (1999). The model is in partial equilibrium because firms take interest rates as given, so this can be considered a model of investment in a small sector or small open economy.

I begin by explaining how the general model applies to this environment.[12] Then, I show how the analytical approach again reveals new insights by deriving a relationship between the KFE for capital gaps and the dynamics of aggregate capital (rather than an average capital gap).

Next, I focus on a specific shock: the arrival of AI, which I model as a permanent increase in the growth rate of productivity. I use the analytical solution to trace the full transition and show how the IRF changes nonlinearly with shock size, highlighting the limits to marginal analysis.

6.1 Environment

The environment is a special case of the investment model in Baley and Blanco (2021). A continuum of competitive firms use capital K and productivity P to produce and sell output Y by

$$Y(P, K) = P^{1-\alpha} K^{\alpha}, \qquad \alpha \in (0, 1)$$

[12] Supplemental Appendix E provides an additional illustration of how the general model maps to this example by documenting the effects of a large productivity shock on the entire dynamic distribution and reset flow path.

Log productivity $p \equiv \log P$ follows

$$dp = g_p dt + \sigma_p dW$$

where W is a Wiener process that is independent across firms.

Firms must pay a fixed cost κP in order to adjust their capital stock, which they can then buy or sell at price q. Inside the inaction region, capital depreciates at rate ζ.

The firm's problem is designed to be homogeneous of degree one, so the state variable reduces to a single dimension, the capital-productivity ratio $\tilde{K} \equiv \frac{K}{P}$. It is convenient to work with log normalized capital $\tilde{k} \equiv \log \tilde{K}$, which diffuses stochastically within the inaction region $[\underline{\tilde{k}}, \bar{\tilde{k}}]$, where the Hamilton-Jacobi-Bellman (HJB) equation is[13]

$$\rho v(\tilde{k}) = e^{\alpha \tilde{k}} + (\mu - \sigma_p^2) v'(\tilde{k}) + \frac{\sigma_p^2}{2} v''(\tilde{k})$$

$$\rho \equiv r - g_p - \frac{\sigma_p^2}{2} \qquad \mu \equiv -(\zeta + g_p)$$

Firms discount cash flows at rate r. The coefficient ρ is the effective discount rate for the normalized HJB. Between adjustments, the law of motion is

$$d\tilde{k} = dk - dp = -(\zeta + g_p)dt - \sigma_p dW = \mu\, dt - \sigma_p dW$$

The value function, boundaries, and optimal reset point must also satisfy the boundary conditions. When transformed in terms of v and $\tilde{k}$, these conditions are:

$$\begin{aligned}
&\text{Value matching} && v(\underline{\tilde{k}}) = v(\tilde{k}^*) - q\left(e^{\tilde{k}^*} - e^{\underline{\tilde{k}}}\right) - \kappa \\
& && v(\bar{\tilde{k}}) = v(\tilde{k}^*) - q\left(e^{\tilde{k}^*} - e^{\bar{\tilde{k}}}\right) - \kappa \\
&\text{Smooth pasting} && v'(\underline{\tilde{k}}) = q e^{\underline{\tilde{k}}} \\
& && v'(\bar{\tilde{k}}) = q e^{\bar{\tilde{k}}} \\
&\text{Optimal reset} && v'(\tilde{k}^*) = q e^{\tilde{k}^*}
\end{aligned}$$

[13] This normalization of the value function and boundary conditions is standard (Stokey, 2008). Supplemental Appendix D documents how to derive this normalized problem.

To map the model to Section 2's state space, define the *capital gap* x as

$$x \equiv \tilde{k} - \underline{\tilde{k}}, \qquad \bar{x} \equiv \bar{\tilde{k}} - \underline{\tilde{k}}, \qquad x^* \equiv \tilde{k}^* - \underline{\tilde{k}}$$

so that x resets to x^*, and inside the inaction region $[0, \bar{x}]$ the distribution of firms follows the KFE (2) with $\gamma = \frac{\sigma_p^2}{2}$ and $\eta = 0$.[14]

To parameterize the model, I measure time in years and choose parameter values to match the capital gap adjustment statistics measured by Baley and Blanco (2021) for Chilean manufacturing firms. First, I choose typical values, setting $\alpha = 0.85$, normalizing $q = 1$, and letting $\zeta = 0.03$ to match the Chilean depreciation rate. Productivity growth is rapid, so I choose a large discount rate $r = 0.16$ in order to keep the firm value finite.[15] Then I choose the remaining parameters to match the average time between adjustments (2.510), average capital gap adjustment (0.239), and variance of adjustments (0.069).[16] This implies the productivity parameters $g_p = 0.065$ and $\sigma_p = 0.190$, and a fixed cost of $\kappa = 14$.

6.2 Aggregation

The density $h(x,t)$ weights each firm equally. Aggregating capital and output instead requires weighting firms by their productivity. Let $f(p,x,t)$ denote the joint density of log productivity and capital gaps, and define aggregate productivity and the productivity-weighted gap density by

$$\begin{aligned} \bar{P}(t) &\equiv \int_0^{\bar{x}} \int_{-\infty}^{\infty} e^p f(p,x,t)\, dp\, dx \\ h_P(x,t) &\equiv \frac{\int_{-\infty}^{\infty} e^p f(p,x,t)\, dp}{\bar{P}(t)} \end{aligned} \tag{20}$$

and thus $\int_0^{\bar{x}} h_P(x,t)\, dx = 1$.

Let $K(t)$ and $Y(t)$ denote aggregate capital and output. I use a P subscript to

[14] This definition of the capital gap is slightly different from that of Baley and Blanco, who define the gap as relative to the steady-state mean rather than $\underline{\tilde{k}}$. I assume zero free adjustments in the baseline, but consider alternatives in Supplemental Appendix F. A low η is necessary for a realistic covariance between adjustments and inaction duration, whereas a large η can match adjustment kurtosis.

[15] This value is close to the large average corporate discount rate measured in the US by Gormsen and Huber (2025).

[16] Supplemental Appendix C derives closed-form expressions for these objects.

denote their values relative to aggregate productivity:

$$K_P(t) \equiv \frac{K(t)}{\bar{P}(t)} = \int_0^{\bar{x}} e^{\tilde{\underline{k}}+x} h_P(x,t)\,dx$$
$$Y_P(t) \equiv \frac{Y(t)}{\bar{P}(t)} = \int_0^{\bar{x}} e^{\alpha(\tilde{\underline{k}}+x)} h_P(x,t)\,dx \tag{21}$$

Thus *detrended* aggregate capital and output are integrals of the weighted density with exponential kernels, that is, of the form (12). Since $\partial_t K = I - \zeta K$ and $\partial_t \bar{P} = g_P \bar{P}$, where $g_P \equiv g_p + \sigma_p^2/2$, detrended aggregate investment satisfies

$$I_P(t) \equiv \frac{I(t)}{\bar{P}(t)} = \partial_t K_P(t) + (g_P + \zeta) K_P(t) \tag{22}$$

The following proposition states a surprising result: the weighted density $h_P(x,t)$ is also a case of the canonical fixed cost problem in Section 2, and thus can be solved and characterized in the same way as the density $h(x,t)$. This is valuable because the entire joint density of productivity and capital is not needed to describe aggregate dynamics.

Proposition 1. *The productivity-weighted gap density satisfies*

$$\partial_t h_P(x,t) = \tfrac{\sigma_p^2}{2}\partial_x^2 h_P(x,t) - \mu_P \partial_x h_P(x,t) + \delta(x - x^*) F_P(t) \qquad \mu_P \equiv \mu - \sigma_p^2 \tag{23}$$

where

$$F_P(t) \equiv \tfrac{\sigma_p^2}{2}\left(\partial_x h_P(0,t) - \partial_x h_P(\bar{x},t)\right)$$

is the productivity-weighted boundary flow. The density is continuous at x^*, satisfies $h_P(0,t) = h_P(\bar{x},t) = 0$, and integrates to one.

Proof: Appendix A.7

A convenient implication of Proposition 1 is that the weighted flow $F_P(t)$ provides a shortcut for deriving aggregate dynamics. By Theorem 2, the Laplace transform of detrended aggregate capital $K_P(t)$ is

$$\hat{K}_P(s) = \hat{A}^{K_P}(s) + \hat{B}^{K_P}(s)\hat{F}_P(s) \tag{24}$$

The proposition also extends Section 5's functional sufficient statistic result. Measuring the empirical objects using productivity weights identifies the marginal IRF

$F_P^{\Delta}(t)$, which then determines the marginal IRF of aggregate capital by equation (24).

6.3 Macroeconomic Effects of Increasing the Productivity Growth Rate

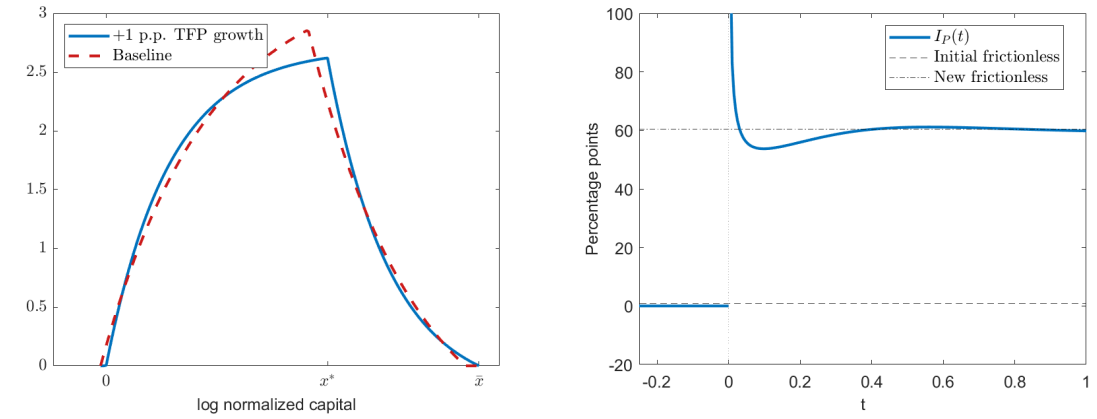
This section considers a timely example: the arrival of AI, which I model as an increase in the growth rate of productivity. As discussed in Section 2.2, the general fixed cost model assumes that inaction boundaries remain fixed. Because the AI shock affects the boundaries, it is a helpful example to show that this paper's method can still be useful in such cases.

Specifically, I study a permanent, unanticipated increase in the growth rate of aggregate productivity. Increasing g_p decreases the drift μ one-for-one, hastening the downward flow of firms' capital gaps. As a result, firms behave differently: they reset normalized capital to a higher level and increase both boundaries and the width of the inaction region.

To analyze the shock using Section 3's framework, initialize the economy in the pre-shock steady state. This becomes the initial distribution, shifted relative to the post-shock inaction region $[0, \bar{x}]$. Some firms will initially be outside the post-shock inaction region; they immediately reset, creating a mass point at x^* in the initial condition $h(x, 0)$. Quantitatively, I increase annual TFP growth $(1 - \alpha)g_p$ by one percentage point. Figure 1a plots the stationary distributions before and after the shock. The change is very small, even though a one-percentage-point increase is large. The inaction boundaries and reset point barely increase, and the shape of the new stationary distribution is nearly unchanged.

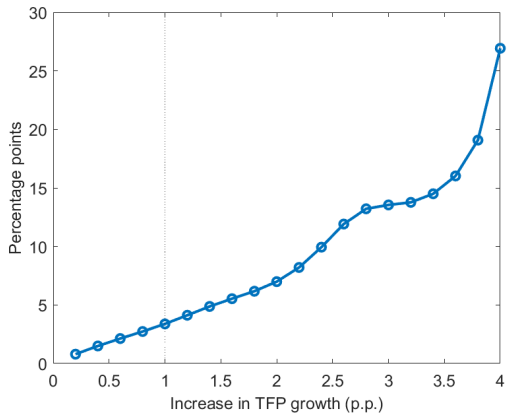
Yet, even though the distribution is mostly unaffected, the shock causes substantial investment dynamics. In a frictionless economy, detrended investment $I_P(t)$ would immediately and permanently increase in response to the shock; Figure 1b plots this level shift with a dashed black line.

In contrast, if there are fixed costs of adjustment, then investment exhibits an immediate boom followed by an extended lull. Figure 1b plots this IRF in blue. The boom occurs because, on impact, the shock shifts the inaction region, raising the lower bound and causing a mass of firms to immediately invest. This boom lingers in the short run as many firms remain close to the new lower bound. The boom then decays into a lull because there is a region near the lower boundary where the initial

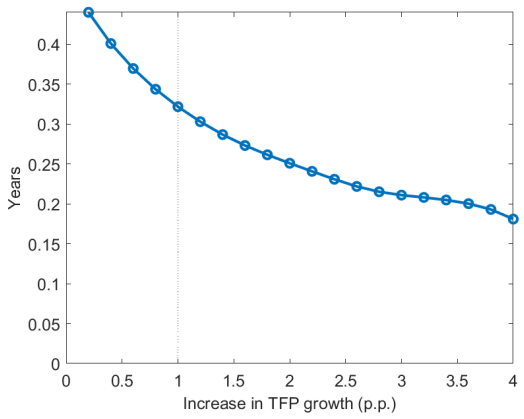


(a) Stationary Distributions

(b) Detrended Investment



(c) Lull Depth



(d) Lull Length

Figure 1: Effects of a Permanent Increase in Productivity Growth

Notes: Time is measured in years. At $t = 0$, the annual growth rate of TFP increases by one percentage point. The upper-left panel compares the stationary distributions of log normalized capital before and after the shock. The upper-right panel plots detrended investment $I_P \equiv I/\bar{P}$ in percentage points relative to its pre-shock steady state. The frictionless investment levels use $\alpha K_{P,f}^{\alpha-1} = (r+\zeta)q$ and $I_{P,f} = (g_P + \zeta)K_{P,f}$. A mass of firms invest at $t = 0$, so the vertical axis is truncated. The lower panels vary the increase in annual TFP growth; dotted vertical lines mark the one-percentage-point baseline. Lull depth is the distance between the post-shock minimum of $I_P(t)$ and its new steady state, as a percent of the steady state. Lull length is the time from the shock until $I_P(t)$ first reaches its new steady state from below after the nadir.

distribution lies below the new steady state, so firms slowly diffuse into this region, partially at the expense of exiting the lower boundary. Eventually, the distribution converges to the new steady state, with aggregate investment only slightly below the frictionless level.

The severity of the investment lull depends on the size of the shock. When the increase in productivity growth is small, the depth of the lull is also small. But Figure 1c documents that larger increases in productivity growth produce deeper lulls. This is because the new steady state shifts more substantially from the initial distribution. However, Figure 1d documents that when the lull depth increases, the length of the lull decreases, so this spell can either be severe and short or mild and protracted.

These dynamics reveal one of the values of the analytical solution: it gives the full IRF, making the boom-lull pattern clear. Moreover, it is easily calculated from the flow $F_P(t)$ without the need to solve the entire distributional dynamics.

Another value of the analytical solution is that it is easily applied to a shock of any size. Many analytical results in the literature are specific to marginal shocks (including Section 5); the full solution complements these methods by easily revealing the effects of shock size. All experiments in Figure 1 begin from the same calibrated steady state but feature different dynamic responses.

7 Conclusion

This paper derives an analytical solution for the dynamic distribution in a canonical fixed cost model. The main insight is to focus on the endogenous reset flow. It can be found without first solving for the distribution and can be used to determine aggregate variables directly. It also reveals new connections between steady-state adjustment behavior and aggregate dynamics.

These results will be valuable in future work, as evidenced by the investment example. For simple models, closed-form expressions are possible, making computation simple and reliable. For more general models, the main insights still apply, including the sufficient-statistic result. The reset flow and Green's function will be useful for thinking about models in any context, and estimating the relevant empirical objects – adjustment flows and the conditional survival function – will be a priority.

References

Adams, Jonathan J., "Sticky Prices for Inflationary Economies: A Tractable Linear Approximation to Menu Cost Models with Trend Inflation," *Federal Reserve Bank of Kansas City Working Paper*, March 2026, *26* (3).

Adams, Jonathan J, Cheng Chen, Min Fang, Takahiro Hattori, and Eugenio Rojas, "Incomplete Information and Irreversible Investment," *Federal Reserve Bank of Kansas City Working Paper No. RWP*, 2025, pp. 25–11.

Alvarez, Fernando and Francesco Lippi, "Price Setting With Menu Cost for Multiproduct Firms," *Econometrica*, 2014, *82* (1), 89–135.

_ and _, "The Analytic Theory of a Monetary Shock," *Econometrica*, 2022, *90* (4), 1655–1680.

_ , Andrea Ferrara, Erwan Gautier, Hervé Le Bihan, and Francesco Lippi, "Empirical Investigation of a Sufficient Statistic for Monetary Shocks," *The Review of Economic Studies*, August 2024, p. rdae082.

_ , Francesco Lippi, and Aleksei Oskolkov, "The Macroeconomics of Sticky Prices with Generalized Hazard Functions," *The Quarterly Journal of Economics*, May 2022, *137* (2), 989–1038.

_ , _ , and Luigi Paciello, "Monetary shocks in models with observation and menu costs," *Journal of the European Economic Association*, April 2018, *16* (2), 353–382.

_ , _ , and Panagiotis Souganidis, "Price Setting With Strategic Complementarities as a Mean Field Game," *Econometrica*, 2023, *91* (6), 2005–2039.

_ , Hervé Le Bihan, and Francesco Lippi, "The Real Effects of Monetary Shocks in Sticky Price Models: A Sufficient Statistic Approach," *American Economic Review*, October 2016, *106* (10), 2817–2851.

Auclert, Adrien, Rodolfo Rigato, Matthew Rognlie, and Ludwig Straub, "New Pricing Models, Same Old Phillips Curves?," *The Quarterly Journal of Economics*, February 2024, *139* (1), 121–186.

Baley, Isaac and Andrés Blanco, "Aggregate Dynamics in Lumpy Economies," *Econometrica*, 2021, *89* (3), 1235–1264.

_ and Julio Andrés Blanco, "The Macroeconomics of Irreversibility," *The Review of Economic Studies*, January 2026, p. rdag001.

Blanco, Andrés and Andrés Drenik, "How Does Inflation "Grease the Wheels" in a Frictional Labor Market?," 2023.

Caballero, Ricardo J. and Eduardo M. R. A. Engel, "Explaining Investment Dynamics in U.S. Manufacturing: A Generalized (S, s) Approach," *Econometrica*, 1999, *67* (4), 783–826.

_ , _ , **and John C. Haltiwanger**, "Plant-Level Adjustment and Aggregate Investment Dynamics," *Brookings Papers on Economic Activity*, 1995, *1995* (2), 1–54.

Caplin, Andrew and John Leahy, "Aggregation and Optimization with State-Dependent Pricing," *Econometrica*, 1997, *65* (3), 601–625.

Caplin, Andrew S. and Daniel F. Spulber, "Menu Costs and the Neutrality of Money*," *The Quarterly Journal of Economics*, November 1987, *102* (4), 703–725.

Cavallo, Alberto, Francesco Lippi, and Ken Miyahara, "Inflation and Misallocation in New Keynesian models," *ECB Forum on Central Banking*, 2023.

_ , _ , **and** _ , "Large Shocks Travel Fast," *American Economic Review: Insights*, 2024.

Cooper, Russell, John Haltiwanger, and Laura Power, "Machine Replacement and the Business Cycle: Lumps and Bumps," *American Economic Review*, 1999, *89* (4), 921–946.

Elsby, Michael W. L. and Ryan Michaels, "Fixed adjustment costs and aggregate fluctuations," *Journal of Monetary Economics*, January 2019, *101*, 128–147.

Evans, Lawrence C, *Partial Differential Equations*, Vol. 19, American Mathematical Society, 2022.

Fisher, Jonas D. M. and Andreas Hornstein, "(S, s) Inventory Policies in General Equilibrium," *The Review of Economic Studies*, 2000, *67* (1), 117–145.

Gertler, Mark and John Leahy, "A Phillips Curve with an Ss Foundation," *Journal of Political Economy*, June 2008, *116* (3), 533–572. Publisher: The University of Chicago Press.

Golosov, Mikhail and Robert E. Lucas Jr., "Menu Costs and Phillips Curves," *Journal of Political Economy*, April 2007, *115* (2), 171–199. Publisher: The University of Chicago Press.

Gormsen, Niels Joachim and Kilian Huber, "Corporate Discount Rates," *American Economic Review*, June 2025, *115* (6), 2001–2049.

Krusell, Per and Jr. Smith Anthony A., "Income and Wealth Heterogeneity in the Macroeconomy," *Journal of Political Economy*, October 1998, *106* (5), 867–896.

Midrigan, Virgiliu, "Menu Costs, Multiproduct Firms, and Aggregate Fluctuations," *Econometrica*, 2011, *79* (4), 1139–1180.

Nakamura, Emi and Jón Steinsson, "Monetary Non-neutrality in a Multisector Menu Cost Model," *The Quarterly Journal of Economics*, August 2010, *125* (3), 961–1013.

Polyanin, Andrei D., *Handbook of Linear Partial Differential Equations for Engineers and Scientists*, New York: Chapman and Hall/CRC, November 2001.

Stokey, Nancy L, *The Economics of Inaction: Stochastic Control Models with Fixed Costs*, Princeton University Press, 2008.

Woodford, Michael, "Information-Constrained State-Dependent Pricing," *Journal of Monetary Economics*, 2009, *56*, S100–S124.

A Proofs

Proofs are written in terms of Section 2.2's generalized model, except for Proposition 1, which is specific to the investment example.

A.1 Proof of Lemma 1

Proof. The boundary and initial conditions follow from the model. It remains to show that $F(t)$ is the intensity of the point source. The homogeneous KFE holds everywhere except at x^*. Its extension to the entire interval has the form

$$\partial_t h(x,t) = \partial_x^2 \left(\gamma(x)h(x,t)\right) - \partial_x \left(\mu(x)h(x,t)\right) - \eta(x)h(x,t) + \delta(x-x^*)R(t)$$

for some unknown function $R(t)$. The Dirac delta $\delta(x-x^*)$ indicates that the residual is only non-zero at x^*. Integrating over $[0,\bar{x}]$ and imposing probability conservation gives

$$\begin{aligned} 0 &= \partial_t \int_0^{\bar{x}} h(x,t)\,dx \\ &= \left[\partial_x \left(\gamma(x)h(x,t)\right) - \mu(x)h(x,t)\right]_0^{\bar{x}} - \int_0^{\bar{x}} \eta(x)h(x,t)\,dx + R(t) \end{aligned}$$

Using the absorbing-boundary conditions, equation (5) implies

$$R(t) = \partial_x \left(\gamma(x)h(x,t)\right)\big|_{x=0} - \partial_x \left(\gamma(x)h(x,t)\right)\big|_{x=\bar{x}} + \int_0^{\bar{x}} \eta(x)h(x,t)\,dx = F(t)$$

For constant coefficients, $\gamma(x) = \gamma$ and $\eta(x) = \eta$, so $\partial_x(\gamma(x)h(x,t)) = \gamma\partial_x h(x,t)$ and $\int_0^{\bar{x}} \eta(x)h(x,t)\,dx = \eta$, which gives the PDE and reset flow in the statement of the lemma. □

A.2 Proof of Theorem 1

Proof. Substitute the eigenfunction expansion of the Green's function into equation (7) and use the definitions of a_n and b_n:

$$\begin{aligned} h(x,t) &= \sum_{n=1}^{\infty} \psi_n^r(x) c_n(t) \\ c_n(t) &\equiv a_n\, e^{-\lambda_n t} + b_n \int_0^t F(\tau)\, e^{-\lambda_n (t-\tau)}\, d\tau \end{aligned} \tag{25}$$

Apply the reset-flow definition in equation (5), then use the definition of θ_n:

$$\begin{aligned} F(t) &= \sum_{n=1}^{\infty} \left(\gamma(0)(\psi_n^r)'(0) - \gamma(\bar{x})(\psi_n^r)'(\bar{x}) + \int_0^{\bar{x}} \eta(x)\psi_n^r(x)\, dx \right) c_n(t) \\ &= \sum_{n=1}^{\infty} \theta_n c_n(t) = \sum_{n=1}^{\infty} \theta_n\, a_n\, e^{-\lambda_n t} + \int_0^t F(\tau) \left(\sum_{n=1}^{\infty} \theta_n\, b_n\, e^{-\lambda_n (t-\tau)} \right) d\tau \end{aligned} \tag{26}$$

Taking the Laplace transform converts the convolution into multiplication:

$$\hat{F}(s) = \sum_{n=1}^{\infty} \frac{\theta_n\, a_n}{s+\lambda_n} + \left(\sum_{n=1}^{\infty} \frac{\theta_n\, b_n}{s+\lambda_n} \right) \hat{F}(s) = \hat{A}(s) + \hat{B}(s)\, \hat{F}(s)$$

Solving this scalar equation for $\hat{F}(s)$ gives the result. □

A.3 Proof of Corollary 1

Proof. Taking the Laplace transform of equation (25) gives

$$\hat{h}(x,s) = \sum_{n=1}^{\infty} \psi_n^r(x)\, \frac{a_n + b_n\, \hat{F}(s)}{s+\lambda_n}$$

Substituting equation (8) gives

$$\hat{h}(x,s) = \sum_{n=1}^{\infty} \psi_n^r(x)\, \frac{\hat{A}(s)\, b_n + \left(1 - \hat{B}(s)\right)\, a_n}{\left(1 - \hat{B}(s)\right)\, (s+\lambda_n)}$$

Equation (26) is a linear Volterra equation that uniquely determines $F(t)$. Conditional on this flow, the KFE is a standard linear parabolic equation with a unique solution (Evans, 2022, Sec. 2.3 Thm. 5).

□

A.4 Proof of Theorem 2

Proof. Corollary 1 gives

$$\hat{h}(x,s) = \sum_{n=1}^{\infty} \psi_n^r(x) \, \frac{a_n + b_n \, \hat{F}(s)}{s + \lambda_n}$$

Taking the Laplace transform of equation (10) and using the definition of θ_n^Z gives

$$\begin{aligned}
\hat{Z}(s) &= \int_0^{\bar{x}} f_Z(x) \, \hat{h}(x,s) \, dx \\
&= \sum_{n=1}^{\infty} \frac{\theta_n^Z \, a_n}{s + \lambda_n} + \hat{F}(s) \sum_{n=1}^{\infty} \frac{\theta_n^Z \, b_n}{s + \lambda_n} \\
&= \hat{A}^Z(s) + \hat{B}^Z(s) \, \hat{F}(s)
\end{aligned}$$

□

A.5 Proof of Corollary 3

Proof. Inverting the partial fraction expansion gives

$$Z(t) = \sum_{j=0}^{\infty} \xi_j^Z \, e^{-\rho_j^Z t}$$

Because $\rho_0^Z = 0$, the $j = 0$ term is $\xi_0^Z = \overline{Z}$. Therefore

$$Z(t) - \overline{Z} = \sum_{j=1}^{\infty} \xi_j^Z \, e^{-\rho_j^Z t}$$

Integrating the impulse response over time gives

$$CIR^Z = \int_0^\infty \left[Z(t) - \overline{Z}\right]\, dt = \sum_{j=1}^{\infty} \frac{\xi_j^Z}{\rho_j^Z}$$

□

A.6 Proof of Theorem 3

Proof. $\bar{h}$ is zero outside $[0, \bar{x}]$. Following a positive shift Δ, the continuous component of the initial measure is $\bar{h}(x - \Delta)$, and the mass that crosses the upper boundary and resets to x^* is

$$M_\Delta = \int_{\bar{x}-\Delta}^{\bar{x}} \bar{h}(y)\, dy$$

The absorbing boundary imposes $\bar{h}(\bar{x}) = 0$, which implies $\frac{d}{d\Delta} M_\Delta \big|_{\Delta=0} = 0$. Thus to first order, the shock causes zero mass to reset, and

$$h^\Delta(x, 0) = -\partial_x \bar{h}(x)$$

The post-shock operator and policy are unchanged, so the marginal density satisfies

$$\partial_t h^\Delta = \mathcal{K} h^\Delta + \delta(x - x^*) F^\Delta(t)$$

and the Green's function is unchanged. Therefore by Property 1

$$h^\Delta(x, t) = -\int_0^{\bar{x}} G(x, y, t) \partial_y \bar{h}(y)\, dy + \int_0^t G(x, x^*, t - \tau) F^\Delta(\tau)\, d\tau$$

Integrating over x, integrating the first term by parts, and using $\bar{h}(0) = \bar{h}(\bar{x}) = 0$ gives

$$0 = \acute{\mathbf{S}}(t) + \int_0^t S(t - \tau \mid x^*) F^\Delta(\tau)\, d\tau$$

where the left-hand side is zero because the marginal perturbation integrates to zero.

Differentiate with respect to t and use $\mathbf{m}(t) = -\partial_t S(t \mid x^*)$ and $S(0 \mid x^*) = 1$ to obtain equation (18). $\acute{\mathbf{S}}(0) = 0$, so its Laplace transform gives equation (19). □

A.7 Proof of Proposition 1

Proof. Away from the reset point, the KFE for the joint density is

$$\partial_t f = -g_p \partial_p f - \mu \partial_x f + \tfrac{\sigma_p^2}{2} \partial_p^2 f + \tfrac{\sigma_p^2}{2} \partial_x^2 f - \sigma_p^2 \partial_{px} f \tag{27}$$

Define $m_P(x,t) \equiv \int_{-\infty}^{\infty} e^p f(p,x,t)\, dp$, so that $h_P = m_P/\bar{P}$. For $x \neq x^*$, equation (27) and integration by parts give

$$\partial_t m_P(x,t) = (g_p + \tfrac{\sigma_p^2}{2}) m_P(x,t) + \tfrac{\sigma_p^2}{2} \partial_x^2 m_P(x,t) - \mu_P \partial_x m_P(x,t)$$

In levels, P follows

$$dP = (g_p + \tfrac{\sigma_p^2}{2}) P\, dt + \sigma_p P\, dW$$

Aggregate productivity grows exogenously by

$$\partial_t \bar{P}(t) = g_P \bar{P}(t)$$

where $g_P \equiv g_p + \sigma_p^2/2$. Differentiating $h_P = m_P/\bar{P}$ with respect to t implies

$$\partial_t h_P(x,t) = \tfrac{\sigma_p^2}{2} \partial_x^2 h_P(x,t) - \mu_P \partial_x h_P(x,t) \qquad x \neq x^*$$

Let $R_P(t)$ denote the unknown reset flow at x^*. Integrate the KFE over x:

$$0 = \tfrac{\sigma_p^2}{2} \left(\partial_x h_P(\bar{x},t) - \partial_x h_P(0,t) \right) + R_P(t) = -F_P(t) + R_P(t)$$

Thus $R_P(t) = F_P(t)$. Finally, the continuity and absorbing boundary conditions for f carry over to h_P. □

Supplemental Appendix

B Formulas

This appendix gives closed-form expressions for the general eigenfunction representation in Sections 3 and 4 under the constant-coefficient model. These formulas make the analytical solution directly computable, but are not required for the general results.

B.1 Eigenfunctions and Reset-Flow Coefficients

Let $\chi \equiv \sqrt{2/\bar{x}}$ and $\nu \equiv \mu/(2\gamma)$. The eigenmodes are

$$\begin{aligned} \psi_n^r(x) &\equiv \chi e^{\nu x} \sin\left(\frac{n\pi x}{\bar{x}}\right) \\ \psi_n^\ell(x) &\equiv \chi e^{-\nu x} \sin\left(\frac{n\pi x}{\bar{x}}\right) \\ \lambda_n &\equiv \frac{\gamma n^2 \pi^2}{\bar{x}^2} + \frac{\mu^2}{4\gamma} + \eta \qquad T_n(t) \equiv e^{-\lambda_n t} \end{aligned} \tag{28}$$

Direct substitution gives

$$\mathcal{K}\psi_n^r(x) = -\lambda_n \psi_n^r(x) \qquad \mathcal{K}^\dagger \psi_n^\ell(x) = -\lambda_n \psi_n^\ell(x)$$

Moreover,

$$\int_0^{\bar{x}} \psi_n^\ell(x)\psi_m^r(x)\, dx = \frac{2}{\bar{x}} \int_0^{\bar{x}} \sin\left(\frac{n\pi x}{\bar{x}}\right) \sin\left(\frac{m\pi x}{\bar{x}}\right)\, dx = \mathbf{1}\{n = m\}$$

Thus the Green's function is

$$G(x, y, t) = \sum_{n=1}^{\infty} \psi_n^r(x)\psi_n^\ell(y) T_n(t)$$

The coefficients in Theorem 1 become

$$\begin{aligned} a_n &= \chi \int_0^{\bar{x}} e^{-\nu y} \sin\left(\frac{n\pi y}{\bar{x}}\right) \phi(y)\, dy \\ b_n &= \chi e^{-\nu x^*} \sin\left(\frac{n\pi x^*}{\bar{x}}\right) \\ m_n &\equiv \int_0^{\bar{x}} \psi_n^r(x)\, dx = \frac{\chi(n\pi/\bar{x})\left(1-(-1)^n e^{\nu\bar{x}}\right)}{\nu^2 + (n\pi/\bar{x})^2} \\ \theta_n^{\partial} &\equiv \gamma\left((\psi_n^r)'(0) - (\psi_n^r)'(\bar{x})\right) = \frac{\gamma\chi n\pi}{\bar{x}}\left(1-(-1)^n e^{\nu\bar{x}}\right) \\ \theta_n &= \theta_n^{\partial} + \eta m_n \end{aligned} \tag{29}$$

The coefficient θ_n^{∂} gives resets at the boundaries, while ηm_n gives random resets. The integral defining a_n is interpreted with respect to the initial measure when it contains a point mass. The conditional distribution and its Laplace transform are

$$h(x,t) = \sum_{n=1}^{\infty} \psi_n^r(x)\left[a_n T_n(t) + b_n \int_0^t F(\tau) T_n(t-\tau)\, d\tau\right]$$

$$\hat{h}(x,s) = \sum_{n=1}^{\infty} \psi_n^r(x) \frac{\hat{A}(s) b_n + (1-\hat{B}(s)) a_n}{(1-\hat{B}(s))(s+\lambda_n)}$$

B.2 Closed-Form Aggregating Coefficients

Proposition 2 gives the θ_n^Z sequence for each of the aggregating function examples described in Section 4.3. These series can be used with Theorem 2 to derive aggregate dynamics.

Proposition 2. *For a function $f_Z(x)$, the corresponding integrating sequence is*

$$\theta_n^Z = \int_0^{\bar{x}} f_Z(x) \sqrt{\frac{2}{\bar{x}}} e^{\frac{\mu}{2\gamma}x} \sin\left(\frac{\pi n x}{\bar{x}}\right) dx$$

Let $\omega_n = \nu^2 + \left(\frac{\pi n}{\bar{x}}\right)^2$. Then:

1. *For the exponential case $f_Z(x) = e^{\epsilon x}$:*

$$\theta_n^Z = \frac{\chi\pi n\left(1-(-1)^n e^{(\epsilon+\nu)\bar{x}}\right)}{\bar{x}\left((\epsilon+\nu)^2 + (\frac{\pi n}{\bar{x}})^2\right)}$$

2. For the linear case $f_Z(x) = x$:

$$\theta_n^Z = \chi \frac{\pi n}{\omega_n} \Big[\frac{2\nu}{\bar{x}\omega_n} \Big((-1)^n e^{\nu \bar{x}} - 1 \Big) - (-1)^n e^{\nu \bar{x}} \Big]$$

3. For the quadratic case $f_Z(x) = x^2$:

$$\theta_n^Z = \chi \frac{\pi n}{\bar{x}\omega_n^3} \Big[(-1)^n e^{\nu \bar{x}} \left(-\omega_n^2 \bar{x}^2 + 4\nu\omega_n \bar{x} - 2 \left(3\nu^2 - \left(\frac{\pi n}{\bar{x}} \right)^2 \right) \right) + 2 \left(3\nu^2 - \left(\frac{\pi n}{\bar{x}} \right)^2 \right) \Big]$$

Proof. By the definition of $\psi_n^r(x)$, the desired sequences are given by

$$\theta_n^Z = \int_0^{\bar{x}} f_Z(x) \chi e^{\nu x} \sin \left(\frac{\pi n x}{\bar{x}} \right) \, dx$$

The following results are standard for exponential-sine integrals:

$$\int e^{cx} \sin(dx) \, dx = \frac{e^{cx}}{c^2 + d^2} [c \sin(dx) - d \cos(dx)] \tag{30}$$

$$\int x e^{cx} \sin(dx) \, dx = \frac{e^{cx}}{(c^2 + d^2)^2} \Big[\sin(dx) \Big(c(c^2 + d^2)x - (c^2 - d^2) \Big) + \cos(dx) \Big(-d(c^2 + d^2)x + 2cd \Big) \Big] \tag{31}$$

$$\int x^2 e^{cx} \sin(dx) \, dx = \frac{e^{cx}}{(c^2 + d^2)^3} \Bigg[\sin(dx) \Big(c(c^2 + d^2)^2 x^2 - 2(c^2 - d^2)(c^2 + d^2)x + 2c(c^2 - 3d^2) \Big) + \cos(dx) \Big(-d(c^2 + d^2)^2 x^2 + 4cd(c^2 + d^2)x - 2d(3c^2 - d^2) \Big) \Bigg] \tag{32}$$

In the exponential case, $f_Z(x) = e^{\epsilon x}$ implies

$$\theta_n^Z = \chi \int_0^{\bar{x}} e^{(\epsilon + \nu)x} \sin \left(\frac{\pi n x}{\bar{x}} \right) \, dx$$

Applying equation (30) with $c = \epsilon + \nu$ and $d = \frac{\pi n}{\bar{x}}$ and evaluating at the limits with

$\sin(\pi n) = 0$ and $\cos(\pi n) = (-1)^n$ gives

$$\theta_n^Z = \chi \frac{\pi n}{\bar{x}\left((\epsilon+\nu)^2 + (\frac{\pi n}{\bar{x}})^2\right)}\left(1 - (-1)^n e^{(\epsilon+\nu)\bar{x}}\right)$$

In the linear case, $f_Z(x) = x$ implies

$$\theta_n^Z = \chi \int_0^{\bar{x}} x e^{\nu x} \sin\left(\frac{\pi n x}{\bar{x}}\right)\, dx$$

Apply equation (31) with $c = \nu$ and $d = \frac{\pi n}{\bar{x}}$, and evaluate at the limits:

$$\chi \int_0^{\bar{x}} x e^{\nu x} \sin\left(\frac{\pi n x}{\bar{x}}\right)\, dx = \chi \frac{\pi n}{\bar{x}\omega_n^2}\Big((-1)^n e^{\nu\bar{x}}\big(2\nu - \omega_n\bar{x}\big) - 2\nu\Big) \tag{33}$$

In the quadratic case, $f_Z(x) = x^2$ implies

$$\theta_n^Z = \chi \int_0^{\bar{x}} x^2 e^{\nu x} \sin\left(\frac{\pi n x}{\bar{x}}\right)\, dx$$

Apply equation (32) and evaluate at the limits:

$$\chi \int_0^{\bar{x}} x^2 e^{\nu x} \sin\left(\frac{\pi n x}{\bar{x}}\right)\, dx =$$
$$\chi \frac{\pi n}{\bar{x}\omega_n^3}\Big[(-1)^n e^{\nu\bar{x}}\left(-\omega_n^2\bar{x}^2 + 4\nu\omega_n\bar{x} - 2\left(3\nu^2 - \left(\frac{\pi n}{\bar{x}}\right)^2\right)\right) + 2\left(3\nu^2 - \left(\frac{\pi n}{\bar{x}}\right)^2\right)\Big]$$

□

C Closed-Form Expressions from the Stationary Distribution

This section derives the stationary distribution with drift and random resets, then uses it to calculate moments of gap adjustments and inaction times.

C.1 The Stationary Distribution

The stationary density $\bar{h}(x) \equiv \lim_{t\to\infty} h(x,t)$ and reset flow $\bar{F} \equiv \lim_{t\to\infty} F(t)$ satisfy the KFE

$$0 = \gamma\partial_x^2\bar{h}(x) - \mu\partial_x\bar{h}(x) - \eta\bar{h}(x) + \delta(x - x^*)\bar{F} \tag{34}$$

with $\bar{h}(0) = \bar{h}(\bar{x}) = 0$ and $\int_0^{\bar{x}} \bar{h}(x)\,dx = 1$.

Taking the limit of the conditional solution in equation (7) gives

$$\bar{h}(x) = \bar{F}\int_0^{\infty} G(x, x^*, t)\,dt \qquad \bar{F} = \left(\int_0^{\bar{x}}\int_0^{\infty} G(x, x^*, t)\,dt\,dx\right)^{-1} \tag{35}$$

$\bar{h}(x)$ is determined by the steady-state flow $\bar{F}$ and is independent of the initial condition. The expression for $\bar{F}$ ensures that $\bar{h}(x)$ integrates to one.

Corollary 4 gives these objects in closed form. Define

$$\nu \equiv \frac{\mu}{2\gamma} \qquad \varrho \equiv \frac{\sqrt{\mu^2 + 4\gamma\eta}}{2\gamma}$$

Corollary 4. *The stationary density is*

$$\bar{h}(x) = \frac{\bar{F}e^{\nu(x-x^*)}}{\gamma\varrho\sinh(\varrho\bar{x})}\begin{cases}\sinh(\varrho x)\sinh\left(\varrho(\bar{x} - x^*)\right) & 0 \le x \le x^* \\ \sinh(\varrho x^*)\sinh\left(\varrho(\bar{x} - x)\right) & x^* \le x \le \bar{x}\end{cases} \tag{36}$$

where

$$\bar{F} = \frac{\eta\sinh(\varrho\bar{x})}{\sinh(\varrho\bar{x}) - e^{-\nu x^*}\sinh\left(\varrho(\bar{x} - x^*)\right) - e^{\nu(\bar{x}-x^*)}\sinh(\varrho x^*)} \tag{37}$$

When $\eta = 0$ or $\varrho = 0$, the expressions in Corollary 4 are understood as their continuous limits.

Proof. Away from x^*, equation (34) is

$$\gamma \bar{h}''(x) - \mu \bar{h}'(x) - \eta \bar{h}(x) = 0$$

Substitute $\bar{h}(x) = e^{\nu x} u(x)$:

$$u''(x) - \varrho^2 u(x) = 0$$

The boundary conditions imply

$$\bar{h}(x) = \begin{cases} A e^{\nu x} \sinh(\varrho x) & 0 \le x \le x^* \\ B e^{\nu x} \sinh\left(\varrho(\bar{x} - x)\right) & x^* \le x \le \bar{x} \end{cases}$$

for some A and B. Continuity at x^* requires

$$A \sinh(\varrho x^*) = B \sinh\left(\varrho(\bar{x} - x^*)\right)$$

Hence for some constant C,

$$\bar{h}(x) = C e^{\nu(x - x^*)} \begin{cases} \sinh(\varrho x) \sinh\left(\varrho(\bar{x} - x^*)\right) & 0 \le x \le x^* \\ \sinh(\varrho x^*) \sinh\left(\varrho(\bar{x} - x)\right) & x^* \le x \le \bar{x} \end{cases} \tag{38}$$

Similar to the outflow at the absorbing boundaries, the probability inflow at x^* must match $\bar{F}$:

$$\gamma \left(\bar{h}'(x^{*-}) - \bar{h}'(x^{*+}) \right) = \bar{F}$$

Differentiating the two components of equation (38) gives

$$\begin{aligned} \bar{h}'(x^{*+}) - \bar{h}'(x^{*-}) = & -C\varrho \left[\sinh(\varrho x^*) \cosh\left(\varrho(\bar{x} - x^*)\right) \right. \\ & \left. + \cosh(\varrho x^*) \sinh\left(\varrho(\bar{x} - x^*)\right) \right] \\ = & -C\varrho \sinh(\varrho \bar{x}) \end{aligned}$$

Therefore

$$C = \frac{\bar{F}}{\gamma \varrho \sinh(\varrho \bar{x})}$$

which proves equation (36).

The derivatives of the density at the boundaries are

$$\gamma \bar{h}'(0) = \bar{F} e^{-\nu x^*} \frac{\sinh\left(\varrho(\bar{x} - x^*)\right)}{\sinh(\varrho \bar{x})} \tag{39}$$

$$-\gamma \bar{h}'(\bar{x}) = \bar{F} e^{\nu(\bar{x} - x^*)} \frac{\sinh(\varrho x^*)}{\sinh(\varrho \bar{x})} \tag{40}$$

Integrating equation (34) over $[0, \bar{x}]$ and using $\int_0^{\bar{x}} \bar{h}(x)\, dx = 1$ gives

$$\bar{F} = \eta + \gamma \bar{h}'(0) - \gamma \bar{h}'(\bar{x})$$

Substituting equations (39) and (40) and solving for $\bar{F}$ gives equation (37). □

C.2 Adjustment and Inaction-Time Moments

This section derives in closed form a number of steady-state moments that are measured in manufacturing data by Baley and Blanco (2021).

Let τ denote the duration between two consecutive adjustments by a single agent in the steady state. Because every adjustment begins a new inaction spell and adjustments occur at rate $\bar{F}$, the average spell duration is

$$\mathbb{E}[\tau] = \frac{1}{\bar{F}} \tag{41}$$

Decomposing equation (3), the shares of adjustments occurring at the lower and upper boundaries are

$$p_0 \equiv \frac{\gamma \bar{h}'(0)}{\bar{F}} = e^{-\nu x^*} \frac{\sinh\left(\varrho(\bar{x} - x^*)\right)}{\sinh(\varrho \bar{x})} \tag{42}$$

$$p_{\bar{x}} \equiv -\frac{\gamma \bar{h}'(\bar{x})}{\bar{F}} = e^{\nu(\bar{x} - x^*)} \frac{\sinh(\varrho x^*)}{\sinh(\varrho \bar{x})} \tag{43}$$

Random adjustments account for the remaining share $\eta / \bar{F}$, so

$$\frac{\eta}{\bar{F}} + p_0 + p_{\bar{x}} = 1$$

Define the signed adjustment from state x as

$$\Delta x \equiv x^* - x$$

An adjustment from the lower boundary has size x^*, an adjustment from the upper boundary has size $x^* - \bar{x}$, and the pre-adjustment state of a randomly adjusting firm has density $\bar{h}(x)$. Define

$$M_j \equiv \int_0^{\bar{x}} (x^* - x)^j \bar{h}(x)\, dx \qquad A_j \equiv \mathbb{E}\left[(\Delta x)^j\right] \qquad M_0 = 1 \tag{44}$$

The raw adjustment moments are therefore

$$A_j = \frac{\eta}{\bar{F}} M_j + p_0 (x^*)^j + p_{\bar{x}} (x^* - \bar{x})^j \tag{45}$$

These moments can be written directly in terms of the stationary density. Let $f_j(x) \equiv (x^* - x)^j$, so $f_j(x^*) = 0$. Multiplying equation (34) by $f_j(x)$ and integrating by parts gives

$$\begin{aligned} \bar{F} A_j &= \eta M_j + \gamma \bar{h}'(0)(x^*)^j - \gamma \bar{h}'(\bar{x})(x^* - \bar{x})^j \\ &= \int_0^{\bar{x}} \left(\gamma f_j''(x) + \mu f_j'(x)\right) \bar{h}(x)\, dx \\ &= j(j-1)\gamma M_{j-2} - j\mu M_{j-1} \end{aligned} \tag{46}$$

for $j \geq 2$. For $j = 1$, the same calculation gives $\bar{F} A_1 = -\mu$. Thus, the first four raw moments are

$$A_1 = -\frac{\mu}{\bar{F}} \tag{47}$$

$$A_2 = \frac{2\gamma - 2\mu M_1}{\bar{F}} \tag{48}$$

$$A_3 = \frac{6\gamma M_1 - 3\mu M_2}{\bar{F}} \tag{49}$$

$$A_4 = \frac{12\gamma M_2 - 4\mu M_3}{\bar{F}} \tag{50}$$

In particular, mean duration and mean adjustment satisfy

$$\mathbb{E}[\Delta x] = -\mu \mathbb{E}[\tau] \tag{51}$$

To derive the joint duration–adjustment moment, define normalized duration

$$\widetilde{\tau} \equiv \frac{\tau}{\mathbb{E}[\tau]}$$

Let $\bar{a}$ denote the average elapsed time since the last adjustment among firms in the stationary cross-section. For a spell of length τ, the average elapsed time is $\tau/2$. Thus

$$\bar{a} \equiv \frac{\mathbb{E}[\tau^2]}{2\mathbb{E}[\tau]} = \frac{\mathbb{E}[\tau]}{2}\left(1 + \mathrm{CV}_\tau^2\right) \qquad \mathrm{CV}_\tau^2 \equiv \frac{\mathrm{Var}(\tau)}{\mathbb{E}[\tau]^2} \tag{52}$$

Let $x(t)$ denote the state t periods after an adjustment, and let $x^- \equiv x(\tau^-)$ denote the state immediately before the next adjustment. Between adjustments, $x(t)$ follows equation (1), beginning from $x(0) = x^*$. Applying Itô's formula to $tx(t)$ and taking expectations gives

$$\begin{aligned}
\mathbb{E}[\tau x^-] &= \mathbb{E}\left[\int_0^\tau x(t)\,dt\right] + \frac{\mu}{2}\mathbb{E}[\tau^2] \\
&= \mathbb{E}[\tau]\int_0^{\bar{x}} x\bar{h}(x)\,dx + \frac{\mu}{2}\mathbb{E}[\tau^2] \\
&= \mathbb{E}[\tau](x^* - M_1) + \frac{\mu}{2}\mathbb{E}[\tau^2]
\end{aligned} \tag{53}$$

The second equality follows because the stationary density records the share of time spent at each state, and the last uses equation (44). Since $\Delta x = x^* - x^-$, equations (52) and (53) imply

$$\mathbb{E}[\widetilde{\tau}\Delta x] = M_1 - \mu\bar{a}$$

Using $\mathbb{E}[\widetilde{\tau}] = 1$ and equation (47), the covariance between normalized duration and adjustment size is therefore

$$\mathrm{Cov}(\widetilde{\tau}, \Delta x) = M_1 + \mu\left(\mathbb{E}[\tau] - \bar{a}\right) = M_1 + \frac{\mu\mathbb{E}[\tau]}{2}\left(1 - \mathrm{CV}_\tau^2\right) \tag{54}$$

The duration moments in equations (52) and (54) can be calculated directly from the within-spell problem. Let $D_j(x) \equiv \mathbb{E}_x[\tau^j]$ and $D_0(x) \equiv 1$. For $j = 1, 2$, the

backward equations are

$$\gamma D_j''(x) + \mu D_j'(x) - \eta D_j(x) = -j D_{j-1}(x),$$
$$D_j(0) = D_j(\bar{x}) = 0 \tag{55}$$

Thus $D_1(x^*) = \mathbb{E}[\tau] = 1/\bar{F}$ and $D_2(x^*) = \mathbb{E}[\tau^2]$.

The variance, standard deviation, fourth central moment, raw fourth-to-second moment ratio, and conventional central kurtosis of gap changes are

$$V_{\Delta x} \equiv A_2 - A_1^2 \tag{56}$$
$$\mathrm{SD}[\Delta x] = \sqrt{V_{\Delta x}} \tag{57}$$
$$C_{4,\Delta x} \equiv A_4 - 4A_1A_3 + 6A_1^2A_2 - 3A_1^4 \tag{58}$$
$$R_{4,\Delta x} \equiv \frac{A_4}{A_2^2} \tag{59}$$
$$\mathrm{Kur}_c[\Delta x] \equiv \frac{C_{4,\Delta x}}{V_{\Delta x}^2} \tag{60}$$

D Normalizing the Investment Problem

This appendix describes how to transform the investment problem with state variables (K, P) into the one-dimensional problem in normalized log capital used in the main text.[17] The derivation first moves from $V(K, P)$ to a value function $\widetilde{V}(\widetilde{K})$ in normalized capital levels, and then to $v(\widetilde{k})$ in logs.

Log productivity follows $dp = g_p\,dt + \sigma_p\,dW$, so productivity in levels follows

$$dP = g_P P\,dt + \sigma_p P\,dW$$

where $g_P \equiv g_p + \frac{\sigma_p^2}{2}$. Inside the inaction region, $dK = -\zeta K\,dt$. If the firm has a free adjustment opportunity, define the post-adjustment value operator by

$$\mathcal{R}V(K, P) \equiv \max_{K' \geq 0} \{V(K', P) - q(K' - K)\}$$

Firms discount at rate r, so their two-dimensional inaction-region HJB is

$$\begin{aligned} rV(K, P) = {} & P^{1-\alpha}K^{\alpha} - \zeta K V_K(K, P) + g_P P V_P(K, P) \\ & + \frac{\sigma_p^2 P^2}{2} V_{PP}(K, P) + \eta\left[\mathcal{R}V(K, P) - V(K, P)\right] \end{aligned} \tag{61}$$

Production, capital expenditure, and the fixed cost are all homogeneous of degree one in (K, P). Therefore, the value function is as well:

$$V(cK, cP) = cV(K, P)$$

for any $c > 0$. Define normalized capital and its value function by

$$\widetilde{K} \equiv \frac{K}{P}, \qquad V(K, P) = PV(\widetilde{K}, 1) = P\widetilde{V}(\widetilde{K}) \tag{62}$$

The derivatives satisfy

$$V_K = \widetilde{V}' \qquad V_P = \widetilde{V} - \widetilde{K}\widetilde{V}' \qquad V_{PP} = \frac{\widetilde{K}^2}{P}\widetilde{V}''$$

[17] This approach is well known; see Stokey (2008) for a textbook treatment. I include it here, using Section 6's notation, for the interested reader.

Homogeneity also implies that the reset point is $K^*(P) = P\widetilde{K}^*$ and that

$$\frac{\mathcal{R}V(K,P)}{P} = \widetilde{V}(\widetilde{K}^*) - q(\widetilde{K}^* - \widetilde{K})$$

Substituting these expressions into equation (61) and dividing by P gives the intermediate normalized HJB

$$\begin{aligned} r\widetilde{V}(\widetilde{K}) = \widetilde{K}^\alpha - \zeta\widetilde{K}\widetilde{V}'(\widetilde{K}) + g_P\left[\widetilde{V}(\widetilde{K}) - \widetilde{K}\widetilde{V}'(\widetilde{K})\right] \\ + \frac{\sigma_p^2}{2}\widetilde{K}^2\widetilde{V}''(\widetilde{K}) \\ + \eta\left[\widetilde{V}(\widetilde{K}^*) - q(\widetilde{K}^* - \widetilde{K}) - \widetilde{V}(\widetilde{K})\right] \end{aligned} \tag{63}$$

This step effectively transforms the discount rate. Moving $g_P\widetilde{V}$ to the left-hand side gives

$$\begin{aligned} \rho\widetilde{V}(\widetilde{K}) = \widetilde{K}^\alpha - (\zeta + g_P)\widetilde{K}\widetilde{V}'(\widetilde{K}) + \frac{\sigma_p^2}{2}\widetilde{K}^2\widetilde{V}''(\widetilde{K}) \\ + \eta\left[\widetilde{V}(\widetilde{K}^*) - q(\widetilde{K}^* - \widetilde{K}) - \widetilde{V}(\widetilde{K})\right] \\ \rho \equiv r - g_P = r - g_p - \frac{\sigma_p^2}{2} \end{aligned} \tag{64}$$

The coefficient ρ is the original discount rate r net of the expected growth rate of productivity.

Define

$$\widetilde{k} \equiv \log\widetilde{K} \qquad v(\widetilde{k}) \equiv \widetilde{V}(e^{\widetilde{k}})$$

The derivatives satisfy

$$v'(\widetilde{k}) = \widetilde{K}\widetilde{V}'(\widetilde{K}) \qquad v''(\widetilde{k}) = \widetilde{K}\widetilde{V}'(\widetilde{K}) + \widetilde{K}^2\widetilde{V}''(\widetilde{K})$$

Using these identities in equation (64) gives

$$\begin{aligned} \rho v(\widetilde{k}) = e^{\alpha\widetilde{k}} + (\mu - \sigma_p^2)v'(\widetilde{k}) + \frac{\sigma_p^2}{2}v''(\widetilde{k}) \\ + \eta\left[v(\widetilde{k}^*) - q\left(e^{\widetilde{k}^*} - e^{\widetilde{k}}\right) - v(\widetilde{k})\right] \\ \mu \equiv -(\zeta + g_p) \end{aligned} \tag{65}$$

The physical law of motion for log normalized capital is

$$d\widetilde{k} = \mu\, dt - \sigma_p\, dW$$

At a costly adjustment, the firm pays κP as well as the net capital expenditure. Homogeneity therefore gives the following five conditions in normalized levels

$$\begin{aligned}
\widetilde{V}(\underline{\widetilde{K}}) &= \widetilde{V}(\widetilde{K}^*) - q(\widetilde{K}^* - \underline{\widetilde{K}}) - \kappa \\
\widetilde{V}(\overline{\widetilde{K}}) &= \widetilde{V}(\widetilde{K}^*) - q(\widetilde{K}^* - \overline{\widetilde{K}}) - \kappa \\
\widetilde{V}'(\underline{\widetilde{K}}) &= \widetilde{V}'(\widetilde{K}^*) = \widetilde{V}'(\overline{\widetilde{K}}) = q
\end{aligned}$$

The first two conditions impose value matching at the adjustment boundaries. The derivative conditions impose smooth pasting at both boundaries and optimality of the common reset point $\widetilde{K}^*$. Since $v'(\widetilde{k}) = \widetilde{K}\widetilde{V}'(\widetilde{K})$, the same five conditions in logs are

$$\begin{aligned}
v(\underline{\widetilde{k}}) &= v(\widetilde{k}^*) - q\left(e^{\widetilde{k}^*} - e^{\underline{\widetilde{k}}}\right) - \kappa \\
v(\overline{\widetilde{k}}) &= v(\widetilde{k}^*) - q\left(e^{\widetilde{k}^*} - e^{\overline{\widetilde{k}}}\right) - \kappa \\
v'(\underline{\widetilde{k}}) &= qe^{\underline{\widetilde{k}}} \\
v'(\widetilde{k}^*) &= qe^{\widetilde{k}^*} \\
v'(\overline{\widetilde{k}}) &= qe^{\overline{\widetilde{k}}}
\end{aligned}$$

E Productivity Level Shocks

This appendix provides an additional example of how the abstract objects in Section 3 map to the investment model in Section 6. I consider an economy in the stationary distribution $\bar{h}(x)$ and a permanent, unanticipated aggregate productivity shock that increases the log productivity of all firms by Δ. The shock reduces log normalized capital, and thus x, by Δ for all firms. I use the calibration reported in Section 6.1.

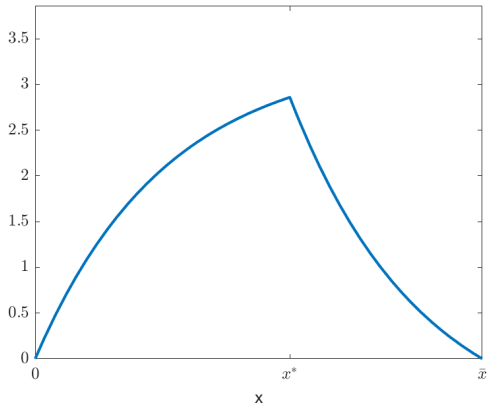
The $\Delta = x^*$ shock pushes the $[0, x^*]$ portion of the stationary distribution (Figure 2a) to the lower bound at $x = 0$. These firms immediately invest in new capital and reset their capital gap to x^*. Thus, the initial condition has a point mass at x^*. The shock also shifts the remaining $[x^*, \bar{x}]$ portion of the stationary distribution to the $[0, \bar{x} - x^*]$ interval. Figure 2b plots the point-mass and density components, which together make up the initial condition $\phi(x) = h(x, 0)$.

Theorem 1 implies that the initial condition is sufficient to solve for $F(t)$, the flow of resetting firms. Figure 2c plots this function. Many firms are near the boundary at $x = 0$ immediately after the shock, so the flow remains high for a while before falling below $\bar{F}$ and then converging back to this long-run value.

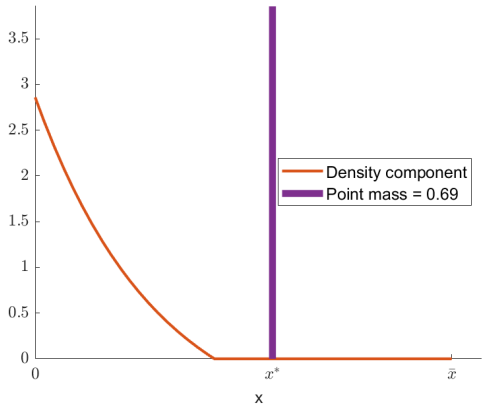
Figure 2d plots the entire distribution. Its evolution explains why the reset flow is non-monotonic. After the shock, many firms are near the boundary at $x = 0$, so the reset flow remains high. These firms quickly diffuse over the boundary and the flow falls. At the same time, the firms that reset on impact are slow to diffuse to either boundary, so the flow falls below its limiting value because most mass is far from the boundaries. In the long run, $h(x, t)$ and the reset flow converge to their stationary values.

The distribution maps the solution to data on firms' states and adjustments, but directly describes only moments such as the average state $X(t)$. Section 6.2 shows that aggregate output and capital can instead be constructed from a productivity-weighted distribution, which can also be solved using Corollary 1.

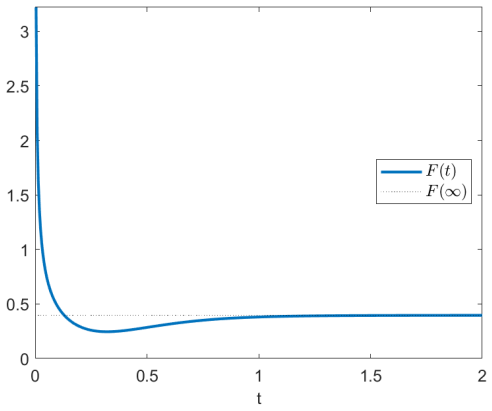
The productivity shock experiment also provides a direct numerical validation of Theorem 3. Figure 3 compares the functional sufficient statistic with exact finite-shock responses. The smallest shocks almost exactly match the theoretical marginal response. The figure also reveals the limits to marginal analysis; the IRF is differently shaped for large shocks, where nonlinearities become quantitatively important.



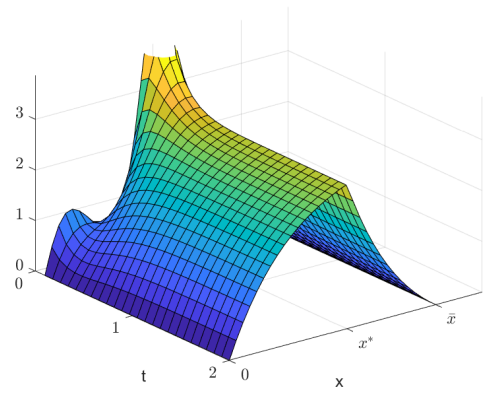
(a) Stationary distribution $h(x, \infty)$



(b) Initial condition $\phi(x)$



(c) Flow of capital-adjusting firms



(d) Dynamic distribution $h(x, t)$

Figure 2: Effects of a Large Productivity Level Shock in the Investment Model

Notes: Time is measured in years. At time $t = 0$, log productivity rises by $\Delta = x^*$. The upper panels plot the stationary distribution and the post-shock initial condition. The lower panels plot the resulting reset flow and dynamic distribution. The dynamic distribution is plotted from $t = 0.10$.

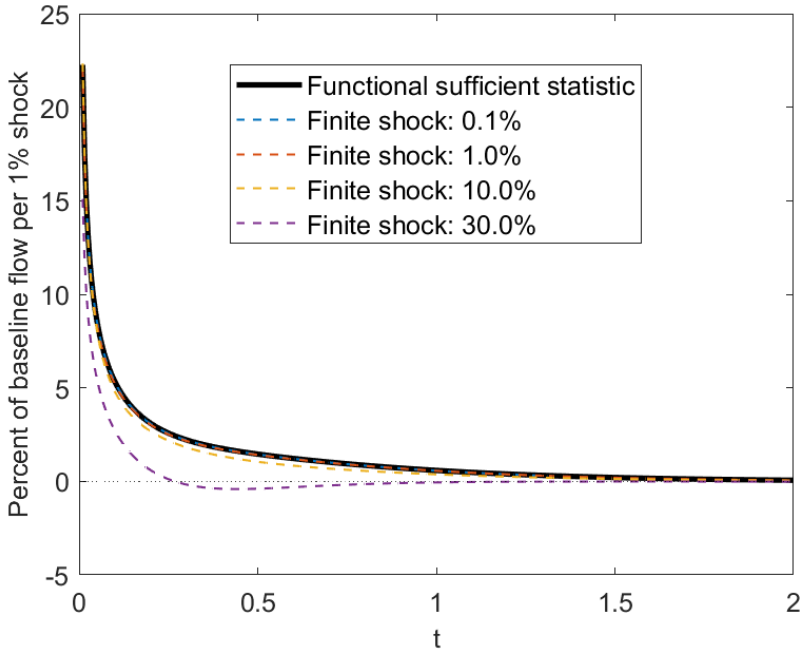


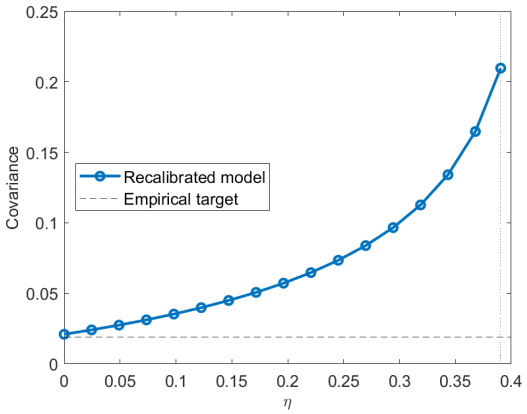
Figure 3: Validating the Functional Sufficient Statistic

Notes: Time is measured in years. The solid black line is the marginal reset-flow response implied by Theorem 3 to a marginal increase in productivity. Colored dashed lines are exact finite-shock responses divided by shock size and rescaled to show the percent change in the reset flow per percent increase in productivity.

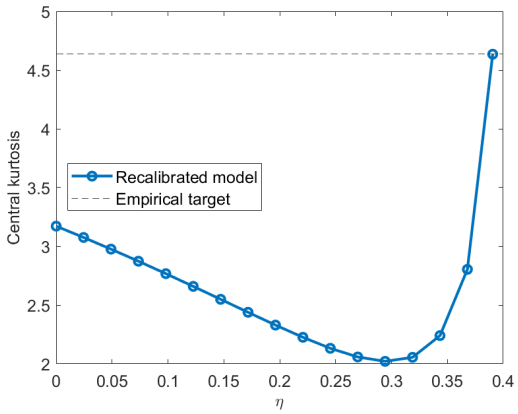
F The Investment Model with Free Adjustments

Section 6's baseline calibration sets $\eta = 0$. To evaluate the effects of introducing free adjustments, this appendix considers alternative values for η. Equation (51) determines μ, and at each η I recalibrate σ_p and κ to match the mean duration and second moment of gap changes exactly.

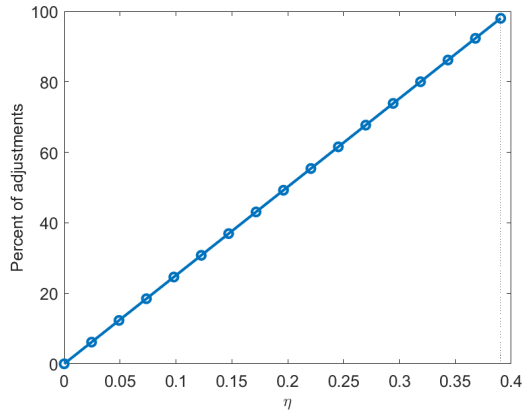
I set $\eta = 0$ in the baseline for both simplicity and realism. Figure 4 reveals why this choice is helpful for describing the data. Figure 4a shows that $\eta = 0$ is the admissible value that most accurately matches the covariance between inaction spell duration and adjustment size. Figure 4b shows that adjustment kurtosis initially falls with η and reaches its empirical target of 4.635 only at $\eta = 0.391$. But at this value, the percentage error in the covariance is enormous: $\text{Cov}(\widetilde{\tau}, \Delta x)$ rises from 0.021 when $\eta = 0$ to 0.210, well above its empirical value of 0.019. Moreover, matching kurtosis implies that the share of free adjustments is 0.980 at this calibration, an extreme value (Figure 4c). Positive free-adjustment rates therefore cannot improve both untargeted moments. Still, Figure 4 shows how the investment IRF to the growth rate shock is affected by alternative calibrations; they change the quantitative transition but preserve the boom-lull investment pattern shown in Figure 1b.



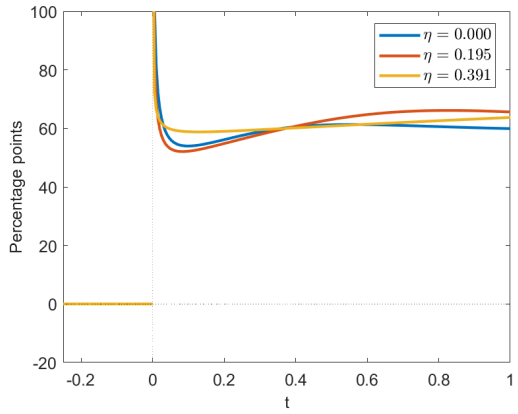
(a) Duration–Adjustment Covariance



(b) Central Kurtosis



(c) Share of Free Adjustments



(d) Investment Responses

Figure 4: Alternative Calibrations with Free Adjustments

Notes: Panels (a)–(c) vary η, recalibrating σ_p and κ at each value. Dashed lines denote the empirical values measured by Baley and Blanco (2021). The dotted vertical lines in panels (a)–(c) mark the value of η that matches adjustment kurtosis. Panel (d) compares detrended investment responses to the one-percentage-point increase in TFP growth for $\eta = 0$, the kurtosis-matching value, and the midpoint. Investment is measured in percentage points relative to its pre-shock steady state, and the impact response is truncated at 100 percentage points.